Journal of Applied Electrochemistry (2005) 35:1203–1211
DOI 10.1007/s10800-005-9028-4

Electrocatalytic activity of copper alloys for NO_3^- reduction in a weakly alkaline solution Part 1: Copper–zinc

Z. MÁCOVÁ and K. BOUZEK*
*Department of Inorganic Technology, Institute of Chemical Technology, Technická 5, 166 28 Prague 6, Czech Republic (*author for correspondence, fax: +420-2-2431-1902, e-mail: bouzekk@vscht.cz)*

Received 18 June 2004; accepted in revised form 18 April 2005

Key words: alloy, copper, electrocatalytic activity, electrochemical reduction, nitrates, zinc

Abstract

A comparative study of the influence of an addition of Zn to Cu as the basic cathode material on electrocatalytic activity for NO_3^- reduction was performed. Potentiodynamic measurements using a rotating ring-disk electrode were carried out in an artificial solution simulating solution after regeneration of the ion-exchange column for NO_3^- removal in drinking water treatment. The results were verified by batch electrolysis experiments. An enhancement of the electrocatalytic activity was observed. Unfortunately, NH_3 was found to be the main NO_3^- reduction product. The highest electrocatalytic activity was obtained using an electrode containing 41 wt.% Zn.

1. Introduction

Interest in NO_3^- removal methods results from the high concentration of NO_3^- in surface and subterranean water streams and the need to reduce this dangerous pollution [1]. The main causes of this pollution are industrial wastewater and, in some areas, intensive agriculture. Another aspect of NO_3^- reduction is the problem of nuclear waste treatment, where NO_3^- significantly increases the volume of waste and has a negative impact on its cohesion after solidification [2]. The syntheses of certain nitrogen compounds or NO_3^- detection by electroanalytical procedures are also of interest [3].

The reduction of the NO_3^- ion is one of the few means of removing it from polluted waters. Both electrochemical and catalysed chemical reduction lead to a relatively broad spectrum of products, such as N_2 gas, NH_2OH, N_2O, NH_3, etc. In electrochemical reduction, the final product composition depends mainly on the electrolyte pH, the applied potential and the cathode material used.

Mass transfer of the NO_3^- ions from the bulk of the solution to the electrode surface limits the application of electrochemical methods in drinking water treatment where the concentration of NO_3^- is typically low. On the other hand, electrochemistry provides a promising solution when combined with ion exchange which is capable of selective removal of NO_3^- from treated water. After regeneration of the ion exchanger, concentrated NO_3^- solutions suitable for electrochemical treatment are produced [4–6].

Many papers dealing with the electrochemical reduction of NO_3^- have been published, the majority dealing with single metal electrodes [7–10]. Recently, binary metal electrodes in the form of alloys [11, 12], co-deposited films [13] or electrodes with foreign adatoms on their surface [14–21] have been studied. This is due to the specific electrocatalytic properties of such materials. The surfaces, consisting of more than one metal, differ from those of the individual constituent materials. This is said to be due to a shift in the binding energy of the atomic core levels [13]. In many cases this results in an enhancement of the desired catalytic properties of the constituent materials.

In relation to binary metal electrodes this effect may also be caused by bifunctional electrocatalysis. The theory of this phenomenon assumes that on one surface constituent a certain reaction step is catalysed and on a second one a different reaction mechanism step, which completes the previous one, takes place. With regard to NO_3^- reduction, for example, this is the reduction of NO_3^- to NO_2^- on Cu and the hydrogenation of NO_2^- to final products on Pt in the case of a Cu/Pt electrode [18].

The best electrochemical activities for NO_3^- reduction have been observed in monometallic electrodes with a Cu [7] cathode in weakly alkaline solutions and with a Rh [8] cathode in acidic solutions. Of the binary electrodes, it is Sn/Pt [20]. Cu/Pd [21] and Cu/Pt [17] also show satisfactory results in acidic media.

The present study concerns alloy electrodes on the basis of Cu and Zn metals. As mentioned above, the

electrochemical activity of Cu for NO_3^- reduction is good, but the reduction leads to NH_3 as the main final product. This would create complications in drinking water treatment even if electrochemical reduction were used as a complementary technique to ion exchange. Another parameter is the kinetics of the reaction. Its enhancement would increase process efficiency. In the literature information about Zn is not so general as in the case of Cu. According to Fanning [2], Zn is used as a chemical reducing agent in various analytical procedures. Li et al. [9] examined the electroreduction of NO_3^- in a strongly alkaline solution on Ni, Pb, Zn and Fe cathodes. Of these, the Zn cathode showed the highest electrocatalytic activity for NO_3^- reduction. Nevertheless, in this case the reaction also leads to NH_3 as the main final product. Keita [22] found that Zn^{2+} addition to the electrolyte had a positive effect on cathodic reduction of NO_2^-, which indicates that Zn is a suitable complementary metal to Cu for the cathode material in terms of the reaction kinetics. Cu catalyses the reduction of NO_3^- to NO_2^- and Zn the reduction of NO_2^- to the final product. In such an arrangement products other than NH_3 could, in principle, be expected.

The cathode alloy materials studied in the literature are typically based on noble metals. This is a very important economic aspect. In order to make electrochemical NO_3^- reduction interesting for broad practical application it is necessary to find a material that preferably does not involve noble metals while also having sufficient electrocatalytic properties. Brass is a viable material produced industrially on a large scale. Nevertheless, it has not yet been studied.

The aim of this paper is to provide a comparative study of the electrocatalytic activity of electrodes with different Cu:Zn ratios for NO_3^- reduction using potentiodynamic measurements with a rotating ring-disk electrode and batch electrolysis. The results obtained permit a conclusion to be derived as to the influence of electrode material composition on the kinetics of NO_3^- reduction and on the selectivity of NO_3^- reduction with respect to the final products.

2. Experimental

2.1. *Apparatus*

Potentiodynamic measurements at a rotating ring-disk electrode (RRDE) PINE AFMSRX were carried out with a PINE bi-potentiostat, model AFCBP 1, controlled by a personal computer with PineChem 2.7.5 software. A two-compartment glass cell was used. A saturated calomel electrode (SCE) connected to the cell by a Luggin capillary served as the reference and all potentials in this paper refer to this electrode. A smooth platinum foil was used as the auxiliary electrode. Platinum was also used as the ring electrode (RE) material. The disk electrode (DE) was exchangeable.

Prior to the experiment both electrodes were polished by emery paper No.: 4000 and washed doubly in demineralised water. The electrocatalytic activity of the Pt ring electrode was tested by potential cycling in sulphuric acid solution. The pure metal (Cu, Zn) electrodes were polarized prior to each experiment for 20 s at 20 mV anodic from the open circuit potential. This was done in order to remove possible surface layers formed during its polarisation in the potential range of H_2 evolution inhibiting NO_3^- reduction. Brass electrodes were left to recover from the inhibition effect. Gradual recovery is possible because Cu hydride is an unstable component. Anodic polarisation was not used in order to minimise the danger of selective electrode dissolution and significant surface composition changes. Polarisation curves were recorded following this procedure until reproducible curves had been obtained.

The cell construction for batch electrolyses was a flow-through electrolyser with a fluidised bed of inert particles in the inter-electrode space and was selected according to the literature [23]. Inert particles (glass spheres) 0.4–0.8 mm in diameter and with 50 % bed expansion enhance the intensity of mass transfer and induce mechanical abrasion of the cathode surface. The electrolyser was equipped with two activated titanium anodes (ATA) and one cathode $0.30 \times 0.06\ m^2$. The cathode was placed in the space between the anodes and its electrochemically active surface area was $0.0336\ m^2$. In this case, too, the potential was measured vs. SCE connected to the cell by a Luggin capillary. Current passing through the cell was recorded by a digital ammeter connected to a personal computer. The electrical charge passed was evaluated by integrating the recorded chronoamperometrical curve.

2.2. *Analytical methods*

During batch electrolyses samples were taken for analysis at regular intervals. At the same time the electrolyte pH was recorded and the electrical charge consumed was measured. The temperature was held at 20 °C.

The NO_3^- content was determined spectrophotometrically at 210 nm wavelength. The analysis was disturbed by HCO_3^- ions, so an appropriate amount of 1 M H_2SO_4 was added to the sample prior to the absorbance measurement [24].

The NO_2^- ion was quantitatively converted to azo dyestuff by the addition of appropriate amounts of CH_3COOH, sulphanilic acid and α-naphthol. Its content was subsequently determined spectrophotometrically at a wavelength of 476 nm [24].

The NH_4^+ ion was converted by Nessler solution ($K_2[HgI_4]$) to a complex compound with highest absorption sensitivity at a wavelength of 380 nm [24].

A UV–Vis–NIR spectrophotometer Cary 50 from Varian was used for spectrophotometric determination of the NO_3^-, NO_2^- and NH_4^+ ion concentrations in the samples.

Cathode material composition was determined using an ARL 9400 XP+ X-Ray fluorescence spectrometer.

2.3. *Chemicals*

All chemicals used were of analytical purity grade. The composition of the solution simulated that of a solution after regeneration of the saturated ion-exchanger, as referred to in [4]. It contained 84.0 g dm^{-3} $NaHCO_3$, 0.4 g dm^{-3} NaCl, 0.4 g dm^{-3} Na_2SO_4 and 1.34 g dm^{-3} $NaNO_3$ (i.e. 1.0 g dm^{-3} NO_3^-) in distilled water. The comparative solution with NO_2^- content contained appropriate amounts of $NaHCO_3$, NaCl and Na_2SO_4 and also 1.11 g dm^{-3} $NaNO_2$ (i.e. 1.0 g dm^{-3} NO_2^-). The pH of freshly prepared electrolyte was 8.3. This did not change during the cyclicvoltammetric experiments. The situation was different in the case of the batch electrolysis, where the ratio of the electrolyte volume to the cathode surface area was substantially lower when compared to the cyclicvoltammetric experiments. Here pH increased during the electrolysis up to 9.2.

The composition of three brass electrodes studied was 30, 35 and 41 wt.% Zn. Pure Cu and Zn were also studied. The brass used for batch electrolyses comprised 35 wt.% Zn.

3. Results

3.1. *Experiments at RRDE*

On the potentiodynamic curves the reactions of interest are to a great extent overlapped by the H_2 evolution reaction, see Figure 1. Due to this the experiments were carried out in a blank electrolyte solution without NO_3^- and NO_2^- ions and then in a solution with NO_3^- or NO_2^- ions present (NO_3^- and NO_2^- experiments, respectively). A polarisation curve of the blank experiment was then subtracted from that measured in the NO_3^- or NO_2^- solution [7]. An identical procedure was used for the current response on the RE. The resulting curve is more transparent, see Figure 2.

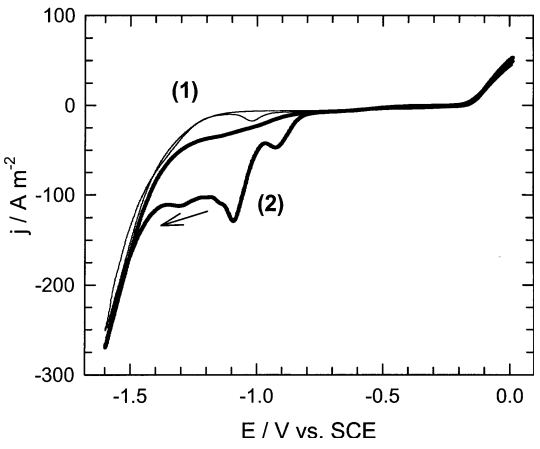

Fig. 1. Comparison of potentiodynamic polarisation curves of a rotating Cu disk electrode in (1) blank electrolyte and (2) electrolyte containing NO_3^-. Potential scan rate 10 mV s^{-1}, electrode rotation rate 19 Hz.

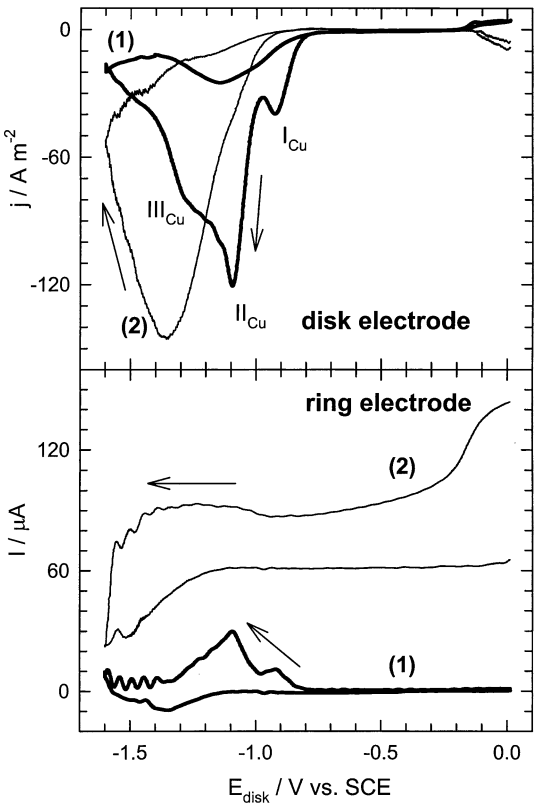

Fig. 2. Subtracted potentiodynamic polarisation curve of a rotating Cu disk electrode and subtracted related current response of a Pt ring electrode at a potential of 1.0 V. Electrolyte solution used: (1) 1 g dm^{-3} NO_3^- and (2) 1 g dm^{-3} NO_2^-; potential scan rate 10 mV s^{-1}, electrode rotation rate 19 Hz. The arrows indicate the potential scan direction of the disk electrode.

3.1.1. *A Cu electrode*

The typical subtracted potentiodynamic curve of the Cu DE in NO_3^- solution, measured between potential limits of 0.01 V and −1.60 V, is given in Figure 2. Three current peaks typical of a Cu cathode (see [7]) can be seen. They are labelled I_{Cu}, II_{Cu} and III_{Cu} here. The reason why the current peaks appear on the polarisation curve instead of a mass transfer limiting current wave or Butler–Volmer type curve typical for RRDE experiments at low potential scan rate is discussed in [7]. As mentioned below, it is assumed, that the cause is inhibition of the NO_3^- reduction reaction at high cathodic potentials by the intense H_2 evolution. This causes the NO_3^- reduction current on the subtracted polarisation curve to fall to zero.

The current response of the Pt RE held at 1.00 V, where oxidation of NO_2^- takes place, belongs to peak I_{Cu} at −0.94 V and peak II_{Cu} at −1.10 V. Current response at lower RE potential was not noted. Peaks I_{Cu} and II_{Cu} therefore correspond to reduction of NO_3^- to NO_2^-. This is in agreement with previous results [7, 25]. Peak III_{Cu} corresponds to a series of reactions of NO_2^- reduction to the final product. These assumptions were proved later on by the batch electrolysis. The reason for

the existence of two peaks (I_{Cu} and II_{Cu}) corresponding to one reaction is not clear yet. Several theories are possible, e.g. the existence of sites on the cathode surface with different binding energies or the influence of the beginning of H_2 production (see next paragraph).

It should be noted that all current peaks almost disappear when the reverse (anodic) potential scan is applied. Similarly to the formation of the current peaks this can be explained in terms of the intensive H_2 evolution taking place in the region of the cathodic vertex potential. Prolonged H_2 evolution leads to inhibition of the Cu surface for the NO_3^- reduction reaction, presumably by the formation of a Cu hydride layer [7].

On the other hand the hysteresis of the current response of the RE is due to blocking of the surface by a significant amount of NH_3 forming at the DE and transported by electrolyte convection to the RE in the DE potential region of peak III_{Cu} [7]. The cathodic vertex potential cannot be moved to the less cathodic potential in order to avoid this interaction because the part of the polarisation curve corresponding to nitrate reduction would be lost.

Similar measurements in the solution containing NO_2^- were carried out. The subtracted potentiodynamic curve obtained at a scan rate of 10 mV s^{-1} is also given in Figure 2 for comparison. It is apparent that peak I_{Cu} vanished completely and the current density of peak II_{Cu} decreased significantly. Compared with the NO_3^- curve, the current density of peak III_{Cu} almost doubled. This confirms the previous statement that this peak corresponds to the reduction of NO_2^- to the final products. The current response of the RE at 1.00 V was in very good agreement with previous results [7].

3.1.2. *The Zn electrode*

The potentiodynamic measurements at the Zn cathode were carried out in the potential range −0.60 V to −1.80 V. The subtracted curve for NO_3^- solution is given in Figure 3. On the DE polarisation curve a slight current wave, labelled I_{Zn}, was observed in the region of −1.45 V. Within the continuing cathodic scan a significant peak, labelled III_{Zn}, appeared at −1.70 V. The anodic scan of the Zn potentiodynamic curve behaved differently from the curve for Cu DE, see Figure 2. The cathodic peaks reached current densities higher than during the cathodic scan. This could be due to activation of the surface within the cathodic scan consisting in the reduction of the surface oxidic layer and/or to the resistance of the Zn cathode surface to inhibition by H_2.

The current response of the Pt RE at a potential of 1.00 V rises at a DE potential of −1.25 V. There is a significant current peak at −1.60 V, which corresponds to both I_{Zn} and III_{Zn}. This did not disappear when lower potentials (0.80 V and 0.60 V) were applied to the RE. The hysteresis of the current response curve during the anodic scan is lower compared to the Cu electrode. This implies that the intermediate and final products are at least partly different from NO_2^- and that NH_3 is not produced with such intensity as on the Cu cathode.

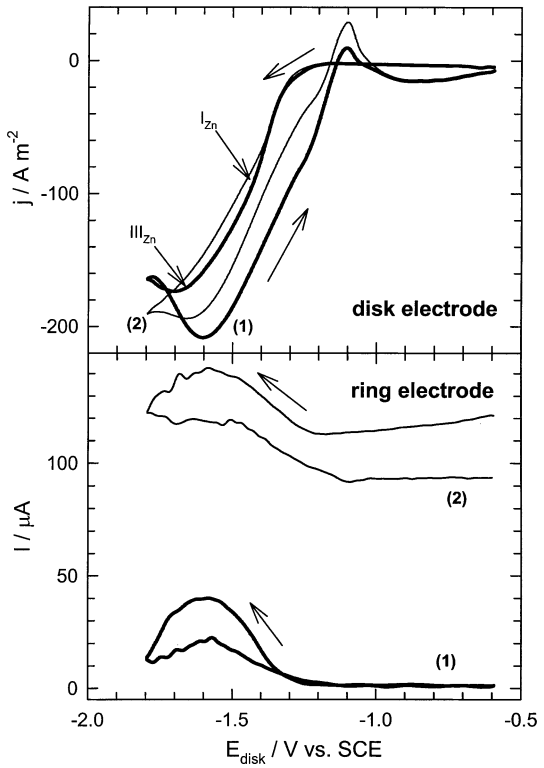

Fig. 3. Subtracted potentiodynamic polarisation curve of a rotating Zn disk electrode and subtracted related current response of a Pt ring electrode at a potential of 1.0 V. Electrolyte solution used: (1) 1 g dm^{-3} NO_3^- and (2) 1 g dm^{-3} NO_2^-; potential scan rate 10 mV s^{-1}, electrode rotation rate 19 Hz. The arrows indicate the potential scan direction of the disk electrode.

The subtracted curve obtained in NO_2^- solution is also shown in Figure 3 for comparison. Peak III_{Zn} does not in fact appear. This is possibly due to the lower sensitivity of Zn to the electrocatalytic activity inhibition by H_2 formed on its surface. The polarisation curve exhibited significant changes with increasing scan rate, see Figure 4. Current density decreased with increasing scan rate. This feature is connected e.g. with a slow chemical reaction step on the cathode surface. Peak III_{Zn} is not observed on either of the polarisation curves.

The shape of the curves measured at individual scan rates is qualitatively identical. The potential scan rate of 500 mV s^{-1} represents an exception. Here a new cathodic peak appears during the cathodic scan at −1.61 V. This can be counted as an independent current peak and it has been marked as II_{Zn}.

The current response at the Pt RE in Figure 3 is qualitatively close for both the NO_3^- and the NO_2^- curve. When curve 1 in Figure 3 is compared with that in Figure 2, it should be noted that the subtracted RE current response did not fall to negative values at the cathodic potential limit and its hysteresis within the anodic scan was low. This demonstrates again the fact that the mechanism of NO_3^- reduction at the Zn cathode differs from that at Cu and products different from NH_3 might be expected.

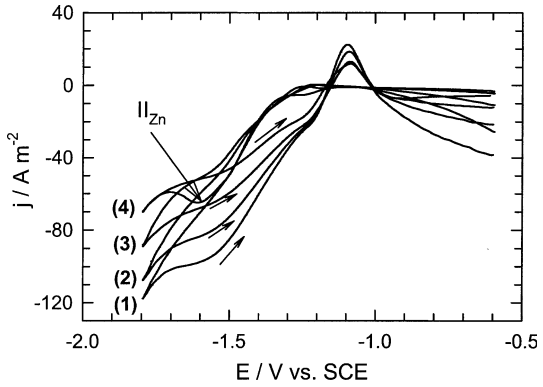

Fig. 4. Subtracted potentiodynamic polarisation curves for a rotating Zn disk electrode. Electrolyte solution used contains 1 g dm^{-3} NO_2^-; potential scan rate: (1) 50 mV s^{-1}, (2) 100 mV s^{-1}, (3) 200 mV s^{-1} and (4) 500 mV s^{-1}, rotation rate of the disk electrode 19 Hz. The arrows indicate the potential scan direction of the disk electrode.

3.1.3. *Cu–Zn alloys*

The Cu alloy electrode containing 41 wt.% Zn was investigated in the potential range −0.25 V to −1.80 V. The polarisation curve obtained (see Figure 5) at a scan rate of 10 mV s^{-1} is characterised by the three current peaks labelled I_{41Zn}, II_{41Zn} and III_{41Zn}. The increase in potential scan rate did not reveal any new peaks. Peaks I_{41Zn} and II_{41Zn} belong to the same potential region as peaks I_{Cu} and II_{Cu} on the Cu curve (Figure 2). Peak III_{41Zn} resembles the polarisation curve of the Zn electrode far more (see Figure 3).

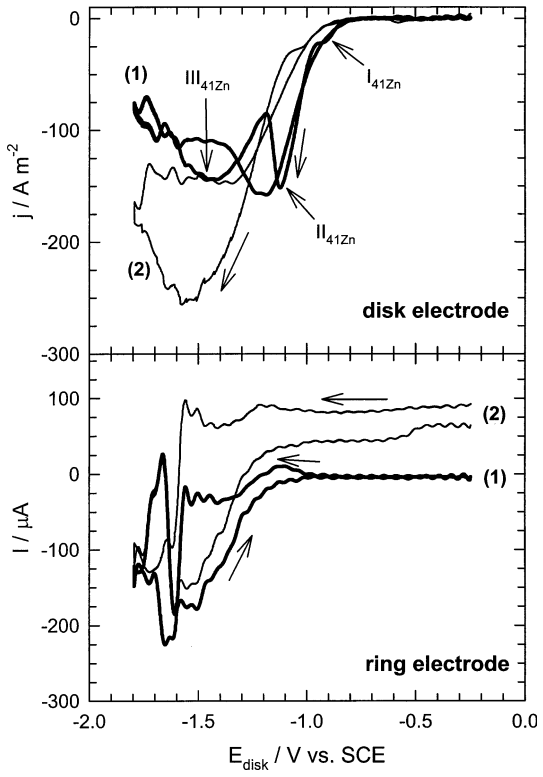

Fig. 5. Subtracted potentiodynamic polarisation curve of a rotating brass disk electrode and subtracted related current response of a Pt ring electrode at a potential of 1.0 V, brass containing 41 wt.% Zn was used. The electrolyte solution used: (1) 1 g dm^{-3} NO_3^- and (2) 1 g dm^{-3} NO_2^-; potential scan rate 10 mV s^{-1}, electrode rotation rate 19 Hz. The arrows indicate the potential scan direction of the disk electrode.

To each of current peaks measured on the DE a corresponding response was found on the RE. This is especially well visible for peaks II_{41Zn} and III_{41Zn}. Close to the cathodic potential limit, in the case of NO_3^- solution, the subtracted RE current response to the DE processes drops to give negative values. According to [7] the cause is poisoning of the Pt surface by NH_3 originating from the DE. The hysteresis of the RE response during the DE anodic potential scan, which confirms the theory about the inhibition of RE by NH_3 evolved at the DE, is detectable. When measurements at lower RE potentials (0.80 V and 0.60 V) were carried out only a current response to peak III_{41Zn} was detected. This confirms the suggestion that this peak is related to the Zn atoms in the alloy and to the mechanism that takes place on the Zn electrode.

In the NO_2^- solution (see Figure 5) peak II_{41Zn}, which corresponds to the reduction of NO_3^- on Cu, disappeared and peak III_{41Zn}, corresponding to the reduction of NO_2^- on Zn, is pronounced. At the RE the oxidation of NO_2^- in the solution took place during all the experiments. Only a slight increase in current was noticed prior to the potential of NO_2^- reduction at the DE (−1.12 V), followed by a rapid decline to the negative values at a DE potential of approximately −1.60 V. This is identical to the RE response in the NO_3^- solution and is also caused by RE poisoning by NH_3 forming at the disk electrode. The steep decline in the RE response for both NO_3^- and NO_2^- reduction indicates that, in both cases, the NO_2^- reduction mechanism is identical. Moreover, it indicates the cathode potential where NH_3 production starts to be significant or where both NO_3^- and NO_2^- are reduced to NH_3 directly without intermediates being transported to the solution. NH_3 is also the reason for the hysteresis of the RE current response.

The polarisation curves measured for the remaining two brass samples are qualitatively very close to those shown in Figure 5 and are therefore not given here. In the case of these cathode materials the RE current response also indicates intensive NH_3 evolution.

3.2. *The kinetic evaluation*

The kinetics were evaluated on the basis of the pseudo-steadystate polarisation curves obtained at different RRDE rotation rates. This approach was chosen because there is no real stationary polarisation curve of NO_3^- reduction to the final product. This is due to the inhibition of the Cu surface by the evolving H_2. Polarisation curves were recorded at scan rates of 5 and 10 mV s^{-1}. They did not differ qualitatively. The current density and potential of the peaks changed due to prolonged exposure to H_2 at the slower scan rate, but the number and character of the current peaks remained unchanged. A scan rate of 10 mV s^{-1} was used during

these experiments. The reason for choosing the higher potential scan rate was shorter exposure of fresh cathode surface to H_2. Koutecky–Levich analysis of the kinetics can be performed under the condition that results will be counted more or less qualitative and they will be used mainly for qualitative comparison of the individual materials [7]. In order to compare the reaction kinetics the potential of the most significant current peaks, corresponding to the reduction of NO_3^- to NO_2^-, was chosen, i.e. peaks II_{Cu}, I_{Zn}, II_{30Zn}, II_{35Zn} and II_{41Zn}. The reason for this choice was that NO_3^- to NO_2^- reduction is generally considered to be the rate-determining step of the whole NO_3^- reduction mechanism.

The resulting Koutecky–Levich plots for brass with 35 wt.% Zn exhibit a non-linear course. For this particular case inverse current density values were extrapolated using a polynomial curve in order to obtain a value of kinetic current density at infinitely fast electrode rotation rate. The results summarised in Table 1 demonstrate that the most electrocatalytically active material among those studied is brass containing 41 wt.% Zn.

3.3. *Batch electrolyses*

Potentiostatic batch electrolyses were carried out in NO_3^- solution. The dependence of the concentrations of the compounds monitored as a function of electrical charge passed is depicted in Figure 6, which also shows the current yield calculated assuming two-step reduction to NH_3 via NO_2^-. The spectrum of possible products and intermediates is broader than just the three mentioned compounds. Therefore a molar balance of the nitrogen was performed. Any difference between nitrogen compound content determined at the start and within the course of the electrolysis allows us to indicate formation of intermediate or final products different from NO_2^- or NH_3.

The current yield of the batch electrolyses at −0.80 V and −0.90 V is very low and NO_3^- ions are converted mainly to NO_2^-. The molar nitrogen balance shows that, at a cathode potential of −0.80 V, approximately 10% of NO_3^- is reduced to compounds different from those currently determined. They are probably reduced to gaseous compound such as N_2.

At a potential of −0.90 V the molar balance showed no nitrogen deficit; thus all reduction products were detected by the analysis. Initially NO_3^- was reduced exclusively to NO_2^- and once the NO_3^- concentration had been reduced to less than half, NH_3 started to be produced.

When a more cathodic potential was applied, the production of NO_2^- was still very high, but in the short term it was accompanied by extensive reduction of NO_2^- to NH_3 until all NO_3^- and NO_2^- had been removed from the solution. The current yield at this potential was much higher than in the case of −0.80 V or −0.90 V. When electrolysis at −1.60 V was carried out only a small concentration level of NO_2^- was obtained (approx. 45 mg dm^{-3}) and current densities of 230 A m^{-2} were achieved. In both cases (−1.10 V and −1.60 V) the molar balance did not show any nitrogen deficit and thus no gaseous products are assumed.

The influence of the use of the brass cathode on its surface composition was followed. As was found by XRF experiments, the composition of a 1 μm thick surface film did not change during 10 electrolyses. Since the electrolysis was reproducible after 3 runs, the composition may be considered stable.

Table 1. The kinetic current densities for NO_3^- reaction determined by Koutecky–Levich analysis; for the brass cathode materials the composition is given as a ratio of the individual component weight percents

	Cathode material				
	Cu	Zn	Cu:Zn = 70:30	Cu:Zn = 65:35	Cu:Zn = 59:41
j_k/A m^{-2}	−120	−115	−125	−140	−185

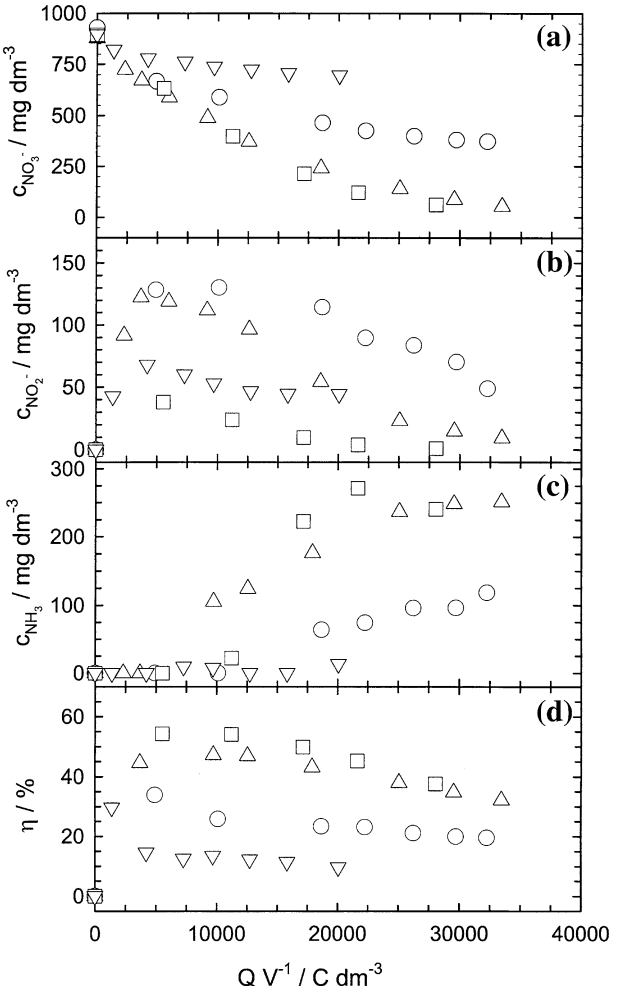

Fig. 6. The dependence of: (a) nitrate, (b) nitrite, (c) ammonium concentrations and (d) current yield on the electrical charge passed during the potentiostatic batch electrolyses. Brass cathode containing 35 wt. % Zn was used. Cathode potentials used: ∇ – −0.80 V, ○ – −0.90 V, △ – −1.10 V and □ – −1.60 V.

4. Discussion

The results summarised in the previous section and Table 1 show that by increasing the content of Zn in the alloy its electrocatalytic activity increased.

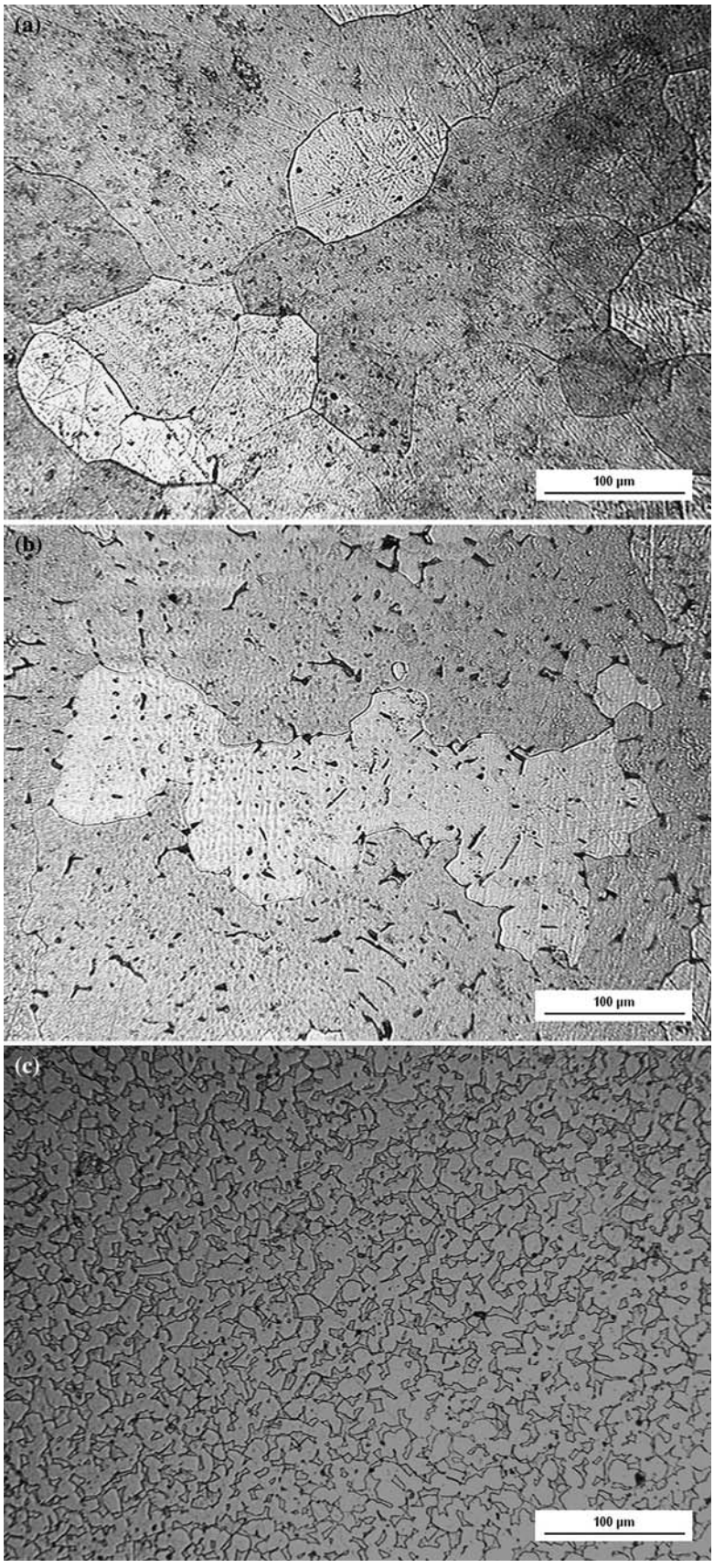

Fig. 7. Metallographic scan of brass with: (a) 30 wt.%, (b) 35 wt.% and (c) 41 wt.% of Zn. Etching agent: 0.2 mol dm^{-3} $FeCl_3$ in 0.2 mol dm^{-3} HCl solution.

According to the phase diagram of Cu–Zn [26], all the materials belong to the same phase composition. Metallographic scans shown in Figure 7 indicate a different situation. In the present case brass containing 30 wt.% Zn consists exclusively of solid solution α. After increase of the Zn content to 35 wt.% a small amount of new phase formed by solution β appears in the structure (dark fields). At the highest Zn content (41 wt.%) the phase β starts to cover a significant part of the brass surface; black dots indicate the presence of Pb. Whereas the solid solution α contains 0–39 wt.% of Zn in Cu, solid solution β is characterised by random distribution of Cu and Zn atoms in the lattice of the Cu–Zn compound. In this phase the Zn content varies in the range 36.8–59.8 wt. %. The reason for the structure being different from that expected from the phase diagram is probably the thermal treatment history of the alloys.

Even the phase structure of the brasses changes with the Zn content, their polarisation curves show similar behaviour. It seems, that phase β has either similar electrocatalytic properties as the prevailing phase α, or that the portion of the surface formed by this phase is still too small to have significant influence. On the other hand, the present results indicate a positive influence of phase β on the kinetics of the NO_3^- reduction.

It is obvious from Table 1, that Zn content below 30 wt.% does not influence the kinetic current density significantly. When it approaches 41 wt.%, increase in the electrocatalytic activity starts to be exponential. This should motivate study of the properties of alloys with higher Zn content. Nevertheless alloys with high Zn content become brittle and unsuitable for practical application. Therefore alloys with Zn content lower than 30 and higher than 41 wt.% were not involved in this study.

The polarisation curve indicates that NO_3^- reduction proceeds in two ways. At lower potentials reduction on the brass cathode is very similar to that on Cu. Peaks I_{30Zn}, I_{35Zn} and I_{41Zn} correspond to peak I_{Cu} and peaks II_{30Zn}, II_{35Zn} and II_{41Zn} can be assigned to peak II_{Cu}. They are therefore connected to NO_3^- reduction to NO_2^-, which was also confirmed by batch electrolysis. The characteristics of peaks III_{30Zn}, III_{35Zn} and III_{41Zn} indicate that the mechanism of NO_2^- reduction is different from that at the Cu electrode. The current responses of the RE confirm this conclusion. This follows especially from the fact that for experiments at anodic RE potentials lower than 1.00 V only a current response to peak III_{41Zn} was obtained.

The potentiodynamic curves of RRDE experiments with a brass DE are very similar in terms of shape. Thus the results of the batch electrolyses executed with an electrode made of material containing 35 wt.% Zn are valid for all Cu–Zn materials presented in this work.

A discrepancy exists between the identification of the potentiodynamic curve peaks (Figure 5) and the results of batch electrolyses (Figure 6). Only NO_2^- should be produced at a potential of −0.90 V (peak II_{41Zn}). However, a significant amount of NH_3 was identified in the electrolyte. The reason is, that the potentiodynamic curve was obtained in the solution free of NO_2^-. On the other hand, the concentration of the NO_2^- exceeded 100 mg dm^{-3} during batch electrolysis. It is further reduced to NH_3.

On the other hand, at the cathode potential of −1.60 V, corresponding to current peak III_{41Zn}, only production of NH_3 is expected. A significant amount of NO_2^- was, however, found in the electrolyte. This can be explained by the RE response shown in Figure 5. At a less cathodic potential than −1.60 V intermediate products may diffuse from the electrode to the solution. Reduction to NH_3 is completed first by their repeated contacts with the electrode surface. At the potential used during electrolysis significant amount of NO_3^- may still be reduced to unspecified intermediates, e.g. NO_2^-.

An interesting feature of the batch electrolyses documented by Figure 6 is the fact that the current efficiency of the NO_3^- reduction process increases as the electrode potential becomes more cathodic. The lowest efficiency observed was for a potential of −0.80 V. In the first instance an attempt was made to explain this behaviour by O_2 reduction. However, as follows from [23], the limiting current density of O_2 reduction under the particular conditions used in the present study has a value of 4.1 A m^{-2}. Thus, in the case of electrolysis at −0.80 V, this represents approximately 30% of average current density (13 A m^{-2}) and at −0.90 V it fell to about 10% of the average. At higher cathode potentials part of the current consumed by the O_2 reduction reaction was negligible. Since the average current efficiency for NO_3^- reduction at the potential of −0.80 V is less than 20%, the O_2 reduction cannot be the only reason for this behaviour. Since an undivided cell is used, an additional possible parasitic reaction is the reoxidation of NO_2^- to NO_3^- on the anode. The average limiting current density corresponding to this reaction is approximately 5.8 A m^{-2}. This was calculated using a mass transfer coefficient for the NO_3^- ion evaluated for an identical experimental cell under identical experimental conditions [23]. Together with the O_2 reduction this represents approximately 75% of the total current. This is in good agreement with the average NO_3^- reduction efficiency observed.

This study has shown that addition of Zn to Cu as the cathode material produced significant enhancement of electrocatalytic activity of the resulting material for NO_3^- reduction. The selectivity of cathode material to final product of the reduction, however, wasn't affected this way.

Acknowledgements

Financial support by Grant Agency of the Czech Republic under project number 106/04/1279 and by the Ministry of Education, Youth and Sports under project number MSM6046137301 is gratefully acknowledged.

References

1. The Nitrate Directive of European Council 91/676/EHS.
2. J.C. Fanning, *Coord. Chem. Rev.* **199**(1) (2000) 159.
3. W.F. Plieth, in A.J. Bard (ed.), 'Nitrogen, in Encyclopedia of Electrochemistry of the Elements', Vol. 8 (Marcel Dekker, New York, 1978), p. 321.
4. Z. Matějka and J. Palatý, CZ patent 284011 B6 (1998).
5. Z. Matějka, D. Nevečeřalová, O. Rejzlová and Š. Gromanová, Advances in Ion Exchange for Industry and Research (The Royal Society at Chemistry, UK, 1999), p. 26.
6. M. Paidar, I. Roušar and K. Bouzek, *J. Appl. Electrochem.* **29**(5) (1999) 611.
7. K. Bouzek, M. Paidar, A. Sadílková and H. Bergmann, *J. Appl. Electrochem.* **31**(11) (2001) 1185.
8. G.E. Dima, A.C.A. de Vooys and M.T.M. Koper, *J. Electroanal. Chem.* **554–555** (2003) 15.
9. H.-L. Li, J.Q. Chambers and D.T. Hobbs, *J. Appl. Electrochem.* **18**(3) (1988) 454.
10. M.C.P. da Cunha, M. Weber and F.C. Nart, *J. Electroanal. Chem.* **414**(2) (1996) 163.
11. M.C.P. da Cunha, J.P.I. De Souza and F.C. Nart, *Langmuir* **16**(2) (2000) 771.
12. Ch. Lu, S. Lu, W. Qiu and Q. Liu, *Electrochim. Acta* **44**(13) (1999) 2193.
13. J.F.E. Gootzen, L. Lefferts and J.A.R. van Veen, *Appl. Catal. A: Gen.* **188**(1–2) (1999) 127.
14. J.F.E. Gootzen, P.G.J.M. Peeters, J.M.B. Dukers, L. Lefferts, W. Visscher and J.A.R. van Veen, *J. Electroanal. Chem.* **434**(1–2) (1997) 171.
15. J.W. Peel, K.J. Reddy, B.P. Sullivan and J.M. Bowen, *Water Res.* **37**(10) (2003) 2512.
16. F.J.G. de Dios, R. Gómez and J.M. Feliu, *Electrochem. Comm.* **3**(11) (2001) 659.
17. O.A. Petrii and T.Y. Safonova, *J. Electroanal. Chem.* **331**(1–2) (1992) 897.
18. T.Y. Safonova and O.A. Petrii, *J. Electroanal. Chem.* **448**(2) (1998) 211.
19. K. Shimazu, T. Kawaguchi and K. Tada, *J. Electroanal. Chem.* **529**(1) (2002) 20.
20. K. Shimazu, R. Goto and K. Tada, *Chem. Lett.* **31**(2) (2002) 204.
21. A.C.A. de Vooys, R.A. van Santen and J.A.R. van Veen, *J. Mol. Catal. A* **154** (2000) 203.
22. B. Keita, I.M. Mbomekalle, L. Nadjo and R. Contant, *Electrochem. Comm.* **3**(6) (2001) 267.
23. M. Paidar, K. Bouzek and H. Bergmann, *Chem. Eng. J.* **85**(2–3) (2002) 99.
24. M. Malát, 'Absorption Inorganic Photometry' (Academia, Prague, 1973), in Czech.
25. J.O'M. Bockris and J. Kim, *J. Electrochem. Soc.* **143**(12) (1996) 3801.
26. A.P. Miodownik, Cu. Zn, in T.B. Massalski (Ed.), 'Binary Alloy Phase Diagrams 2', 2nd edition (William Scott W., Jr., 1990), p. 1508.